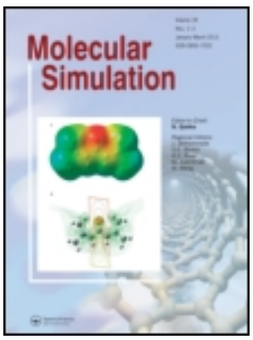

Molecular Simulation

ISSN: 0892-7022 (Print) 1029-0435 (Online) Journal homepage: https://www.tandfonline.com/loi/gmos20

A comparative study of critical temperature estimation of atomic fluid and chain molecules using fourth-order Binder cumulant and simplified scaling laws

Sudhir K. Singh & Jayant K. Singh

To cite this article: Sudhir K. Singh & Jayant K. Singh (2013) A comparative study of critical temperature estimation of atomic fluid and chain molecules using fourth-order Binder cumulant and simplified scaling laws, Molecular Simulation, 39:2, 154-159, DOI: 10.1080/08927022.2012.708755

To link to this article: https://doi.org/10.1080/08927022.2012.708755

Molecular Simulation
Vol. 39, No. 2, February 2013, 154–159

Taylor & Francis
Taylor & Francis Group

A comparative study of critical temperature estimation of atomic fluid and chain molecules using fourth-order Binder cumulant and simplified scaling laws

Sudhir K. Singh[a]*[1] and Jayant K. Singh[b2]

[a]*Department of Chemical Engineering, Institute of Chemical Technology Mumbai, Mumbai 400019, India;* [b]*Department of Chemical Engineering, Indian Institute of Technology Kanpur, Kanpur 208016, India*

(*Received 3 April 2012; final version received 28 June 2012*)

Grand-canonical transition-matrix Monte Carlo simulation with histogram reweighting and finite-size scaling technique are used to calculate fourth-order Binder cumulant of order parameter along the vapour–liquid coexistence line to calculate the critical temperature of bulk and confined square-well fluid in slit pore of two pore sizes. Further, this approach is utilised to estimate the critical temperatures of relatively more complex fluids such as *n*-alkanes confined in graphite and mica slit pores of different slit widths. The estimated critical temperatures are compared with the critical temperature obtained for the same systems using simplified form of the scaling law. This investigation reveals that critical temperatures of simple and complex fluids in bulk state and under confinement, estimated using the scaling law, are within reasonable accuracy with that obtained using more accurate and rigorous approach of fourth-order Binder's cumulant.

Keywords: grand canonical; Binder cumulant; crtitical temperature; slit pore; alkanes

1. Introduction

Computer simulation techniques such as Monte Carlo and molecular dynamics methods yield numerically exact information (apart from statistical errors) on model systems of classical statistical mechanics. However, a systematic limitation is the restriction to a finite particle number or system size. This limitation is particularly restrictive near critical points. However, these finite size effects can also be used as a tool for the quantitative study of phase transitions and critical phenomena [1]. Critical temperature of confined fluids depends on two major factors: (1) the range and strength of attractive and repulsive interactions and (2) the dimensionality or pore width of the system under investigation [2,3]. Unfortunately, in the vicinity of the critical point, computer simulations cannot give accurate results due to the finite size effects, which do not allow taking into account the long-range density fluctuations [4]. Hence, several methods have been devised to estimate the critical temperature on the basis of analysis of numerical data obtained from simulations. Major methods that have been applied for bulk, confined and 2D fluids include mixed-field finite-size scaling technique [5–9], simplified form of scaling law of density [2,3,10] and fourth-order Binder cumulant approach [11–13]. Undoubtedly, mixed-field technique and fourth-order cumulant approach are more rigorous techniques for critical temperature estimation. Moreover, it has been shown in earlier investigations that for realistic intermolecular potentials, the combination of histogram reweighting techniques with the Binder fourth-order cumulant calculation is completely equivalent to the mixed-field method and can be employed in a finite system size study in order to estimate the critical parameters with the same precision as for the mixed-field studies [14].

To our best knowledge, the literature lacks comparison of critical temperature estimates via different approaches for confined fluids, in particular, chain molecules such as alkanes. This work is to fill the gap. In this work, we have compared the critical temperature estimation of simple and complex fluids in bulk and confined states obtained from two methods, viz. simplified form of scaling law of density [2,3] and fourth-order cumulant approach [11]. For the sake of appropriate comparison, square-well fluid is a representative simple fluid. On the other hand, we have considered alkane as an example of relatively complex fluids. As for confinement, we have considered slit pore with smooth walls and atomistically detailed graphite and mica pores. The former is used to confine a square-well fluid and the latter are used for the alkanes (*n*-butane and *n*-octane).

This paper is organised as follows. Section 2 provides a short description of methodology, fluid and surface potential models, information concerning model parameters of the simulation and the critical temperature estimation techniques used in this work. The results obtained in this work are described in Section 3, followed by conclusions in Section 4.

*Corresponding author. Email: sksingh@thapar.edu

ISSN 0892-7022 print/ISSN 1029-0435 online

http://dx.doi.org/10.1080/08927022.2012.708755
http://www.tandfonline.com

2. Simulation methodology, potential models and critical temperature estimation technique

We have employed grand-canonical transition-'matrix Monte Carlo (GC-TMMC) simulation technique [2,3] mainly due to ease of utilising the parallel processors and efficiency over other Monte Carlo techniques [15]. GC-TMMC simulations are conducted in a grand-canonical ensemble. The macroscopic probability is calculated by summing all the microstates at a constant number of molecules. A book keeping scheme of the transition matrix is employed to obtain the macroscopic probability. In this scheme, for each Monte Carlo move we record the acceptance probability in a matrix, regardless of whether the move is being accepted or not. In the current grand-canonical simulation work, the transition probability matrix is tridiagonal. Moreover, to ensure a uniform sampling across all densities, we have employed multi-canonical sampling scheme. Histogram-reweighting method is utilised to obtain the coexistence chemical potential. At a given coexistence of chemical potential, we could observe two peaks in the macrostate probability distribution. The detail method of GC-TMMC technique is described elsewhere [16,17]. We have studied two different model fluids: square-well potential model for simple spherical molecule and modified Buckingham exponential potential model [18] for chain-like molecules such as *n*-alkanes. The confining surfaces for the considered model fluids are smooth and structureless, modelled with square-well potential for confined square-well fluid molecules and by 9-3 potential [19] for confined *n*-alkanes. Models and simulation details are as follows.

2.1 Potential models and simulation details

Fluid–fluid interaction and wall–fluid interaction for square-well potentials are represented by the following expressions:

$$u_{\mathrm{ff}}(r) = \begin{cases} \infty, & 0 < r < \sigma_{\mathrm{ff}}, \\ -\varepsilon_{\mathrm{ff}}, & \sigma_{\mathrm{ff}} \le r < \lambda_{\mathrm{ff}}\sigma_{\mathrm{ff}}, \\ 0, & \lambda_{\mathrm{ff}}\sigma_{\mathrm{ff}} \le r, \end{cases}$$

$$u_{\mathrm{wf}}(z) = \begin{cases} \infty, & 0 < z < \frac{\sigma_{\mathrm{ff}}}{2}, \\ -\varepsilon_{\mathrm{wf}}, & \frac{\sigma_{\mathrm{ff}}}{2} \le z < \lambda_{\mathrm{wf}}\sigma_{\mathrm{ff}}, \\ 0, & \lambda_{\mathrm{wf}}\sigma_{\mathrm{ff}} \le z, \end{cases} \qquad (1)$$

where r is the inter-particle separation distance, z is the separation distance of the particle from the surface, $\lambda_{\mathrm{ff}}\sigma_{\mathrm{ff}}$ is the fluid–fluid potential well diameter, $\varepsilon_{\mathrm{ff}}$ is the depth of the fluid–fluid potential well, σ_{ff} is the diameter of the fluid–fluid hard core, $\lambda_{\mathrm{wf}}\sigma_{\mathrm{ff}}$ is the fluid–wall potential well diameter and $\varepsilon_{\mathrm{wf}}$ is the depth of the fluid–wall potential. All quantities reported in the rest of the article are made a dimensional using characteristic energy, $\varepsilon_{\mathrm{ff}}$, and length scale, σ_{ff}. For example, temperature is reduced by $\varepsilon_{\mathrm{ff}}/k$. The parameters, λ_{ff}, λ_{wf}, $\varepsilon_{\mathrm{ff}}$ and $\varepsilon_{\mathrm{wf}}$, are kept 1.5, 1.0, 1.0 and 4.0, respectively.

A united-atom approach [20] is used to model the *n*-alkane molecules. Non-bonded site–site interactions are described with the modified Buckingham exponential intermolecular potential [18], for which pair interaction energy, U, is represented as

$$U(r) = \left\{ \frac{\varepsilon}{1-6/\alpha} \left[\frac{6}{\alpha} \exp\left(\alpha \left[1 - \frac{r}{r_{\mathrm{m}}} \right] \right) - \left(\frac{r_{\mathrm{m}}}{r} \right)^6 \right] \right\}, \quad \text{for } r > r_{\max},$$
$$U(r) = \infty, \quad \text{for } r < r_{\max}, \qquad (2)$$

where ε, r_{m} and α are adjustable parameters. The variable r_{m} is the radial distance at which $U(r)$ reaches a minimum and the cut-off distance $r_{\max}$ represents the smallest radial distance for which $d(U(r))/d(r) = 0$. The radial distance for which $U(r) = 0$ is denoted by σ. The parameters ε, σ and α are 129.63 K, 3.679 Å and 16, respectively, for the methyl group (—CH_3) and 73.5 K, 4.00 Å and 22, respectively, for the methylene group (—CH_2—). The other details related to cross-parameter evaluation, bond bending angle and torsion angle potential and related parameters are reported and taken from Ref. [2]. The wall–fluid interaction for the graphite and mica surfaces with *n*-alkane molecule are described by the 9-3 potential [19], given as

$$\phi_{\mathrm{wf}}(z) = \frac{2}{3}\pi\rho_{\mathrm{w}}\varepsilon_{\mathrm{wf}}\sigma_{\mathrm{wf}}^3 \left\{ \frac{2}{15}\left(\frac{\sigma_{\mathrm{wf}}}{z} \right)^9 - \left(\frac{\sigma_{\mathrm{wf}}}{z} \right)^3 \right\}, \qquad (3)$$

where z is the distance of the fluid particle from the wall and ρ_{w}, $\varepsilon_{\mathrm{wf}}$ and σ_{wf} are the parameters of the 9-3 potential. In Equation (3), $\sigma_{\mathrm{wf}} = (\sigma_{\mathrm{w}} + \sigma_{\mathrm{ii}})/2$, where σ_{w} denotes 'diameter' of a wall atom and σ_{ii} refers to the molecular diameter of corresponding CH_2—CH_2 or CH_3—CH_3— interactions. Potential parameters, ρ_{w}, $\varepsilon_{\mathrm{wf}}$ and σ_{w}, for graphite and mica surfaces can be seen in Ref. [2].

In this work, grand-canonical simulations are conducted with 30% displacement and 70% insertion/deletion moves for the square-well model system. For the phase coexistence simulations of the bulk square-well fluid, box sizes were varied discretely from 10 to 20 molecular diameters. On the other hand, for slit width, $H = 8$ the box edge length along the unrestricted directions was varied discretely from 8 to 15 molecular diameters and for $H = 2$ it was varied from 28 to 50 molecular diameters. Further, for confined *n*-alkanes, configurational-bias grand-canonical simulations are conducted with 15% particle displacement, 50% particle insertion/deletion, 15% particle rotation and 20% particle regrowth. For the phase coexistence simulation, box sizes for *n*-butane confined in 20 Å slit width were varied in unrestricted directions from 50 to 100 Å. However, box sizes for

n-octane confined in 30 Å slit width were varied from 70 to 110 Å. The simulation run lengths were varied from 10 to 100 h depending on the type of molecule and nature of confinement under investigation, on Intel core Xeon processor having eight central processing units.

2.2 Critical temperature estimation techniques

We have considered two different techniques for critical temperature estimation using data obtained from GC-TMMC simulations. Importantly, in the close vicinity of the critical point, the characteristic size of the density fluctuations increases, hence the simulation cannot be performed near the critical point. Wegner [21] showed that away from the critical point, the difference in coexisting vapour and liquid densities can be written in the following form:

$$\rho_{\mathrm{l}} - \rho_{\mathrm{v}} = C_0\left(1 - \frac{T}{T_{\mathrm{c}}}\right)^{\beta} + C_1\left(1 - \frac{T}{T_{\mathrm{c}}}\right)^{\beta+\Delta} + C_2\left(1 - \frac{T}{T_{\mathrm{c}}}\right)^{\beta+2\Delta} + \cdots, \tag{4}$$

where ρ_{l}, ρ_{v} and T_{c} are coexistence liquid and vapour number densities and critical temperature, respectively; Δ is the gap exponent and C_i are the correction amplitude or coefficients. The parameter β is known as the order parameter critical exponent. However, for the temperatures, T, moderately close to critical point, $0 < (1 - (T/T_{\mathrm{c}})) < 0.2$, the gap exponent terms which describe behaviour far away from the critical point were expected to be very small as compared to other leading terms [21]. Moreover, all the higher terms C_i for $i > 0$ in the Wegner expansion, i.e. in Equation (4), can be excluded without any significant change in the estimated critical temperature, T_{c}. Therefore, the estimation of the T_{c} is generally based on the knowledge of several liquid–vapour coexistence points obtained from GC-TMMC simulations in an appropriate temperature range. Further, using the following simplified form of Equation (4), T_{c} is estimated as

$$\rho_{\mathrm{l}} - \rho_{\mathrm{v}} = C_0\left(1 - \frac{T}{T_{\mathrm{c}}}\right)^{\beta}. \tag{5}$$

Another more rigorous technique for estimation of T_{c} is based on Binder's fourth-order cumulant, U_L, given by the following expression:

$$U_L = 1 - \frac{\langle M^4\rangle_L}{3\langle M^2\rangle_L^2}, \tag{6}$$

where M is the deviation from the mean density, i.e. $\rho - \langle\rho\rangle$. The $\langle M^2\rangle$ and $\langle M^4\rangle$ denote the second and fourth moments of the order parameter. The cumulant, U_L, at the critical point would be a universal point [11].

The idea behind this technique is to record the U_L along the vapour–liquid saturation curve at different temperatures near a guessed critical temperature for different system sizes, L. For temperatures $T > T_{\mathrm{c}}$, fourth-order cumulant, U_L, decreases to zero as U_L is proportional to L^{-d}, where d is the dimensionality of the system. On the other hand, for $T < T_{\mathrm{c}}$, U_L tends to $U_\infty = 2/3$. Thus, for a system size $L' > L$ and any $T < T_{\mathrm{c}}$ we shall get $U_{L'} > U_L$ and if $T > T_{\mathrm{c}}$, then $U_{L'} < U_L$. This behaviour of the cumulant makes it very useful for obtaining the estimate of T_{c}. In this study, we have used the guessed critical temperature estimated in our earlier work [2,3,22], using simplified form of scaling law. To evaluate it, U_L is calculated for different temperatures and is plotted against temperature for different system sizes, L. The plots of U_L for different L would ideally or theoretically have a common intersection point. However, practically at least their intersection would be fairly close, corresponding to the critical temperature of an infinite system [11,23]. Moreover, by computer simulation which is a practical approach, it is not possible to get a unique/common intersection point corresponding to the critical temperature. In such cases, critical temperature is estimated by taking average of the intersection points which are fairly close in the current investigations, as shown in Figures 1–3.

3. Results and discussion

We start our discussion with critical temperature estimation of monatomic fluid in bulk and confined states using a finite-size scaling technique of fourth-order Binder cumulant, U_L. As an example, we have taken square-well fluid as a candidate for this study.

Figure 1(a)–(c) shows U_L of the order parameter as the function of temperature, T, calculated along the vapour–liquid coexistence curve, for a bulk square well and the fluid confined in attractive slit pore of widths, $H = 8$ and 2 molecular diameters, respectively. Critical temperature, T_{c}, of bulk square-well fluid estimated using fourth-order cumulant technique is around 1.217 ± 0.002 as reported in Table 1. On the other hand, the critical temperature for the studied bulk square-well fluid estimated in earlier work [3] using simplified form of scaling law is around 1.219 ± 0.001. Figure 1(b),(c) displays T_{c} for $H = 8$ and 2, respectively, using cumulant approach. T_{c} estimated using cumulant approach for $H = 8$ and 2 are 1.097 ± 0.006 and 0.734 ± 0.001, respectively, as also reported in Table 1. On the other hand, T_{c} for $H = 8$ and 2, estimated using simplified form of scaling law reported in the earlier work [2], are 1.091 ± 0.004 and 0.745 ± 0.002, respectively, also reported in Table 1. This indicates that, with respect to cumulant approach, the difference in the estimated critical temperature using simplified form of

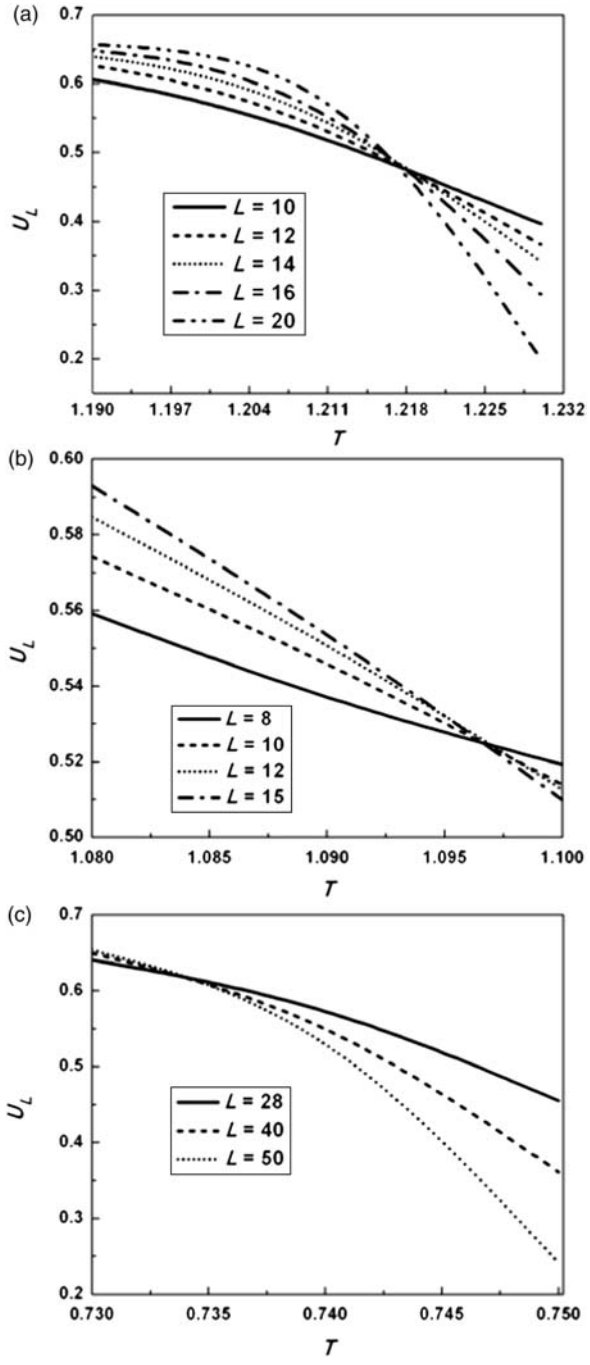

Figure 1. The fourth-order cumulants, U_L of order parameter, estimated along vapour−liquid coexistence curve plotted as a function of temperature, T, for different system sizes, L. (a−c) Approach is demonstrated with a typical square-well fluid in bulk and confined in attractive slit pore of width, $H = 8$ and 2 molecular diameters, respectively. The U_L is estimated at discrete temperatures in the range $1.19 \leq T \leq 1.23$, $1.08 \leq T \leq 1.1$ and $0.73 \leq T \leq 0.75$ for the cases (a), (b) and (c), respectively.

scaling law and cumulant approach for bulk square-well fluid is less than 0.16%, whereas for $H = 8$ and 2 this difference is less than 0.6% and 1.5%, respectively. This

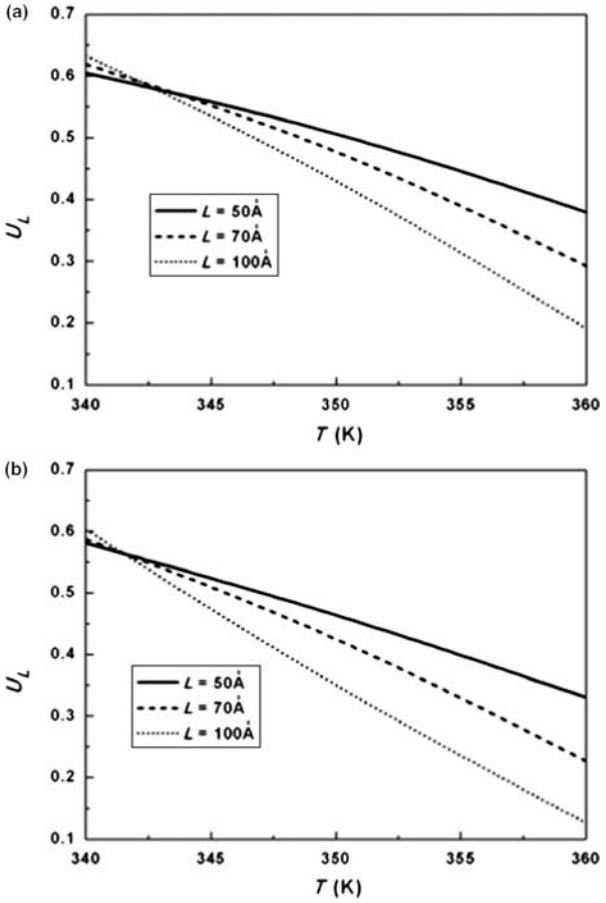

Figure 2. The fourth-order cumulants, U_L of order parameter, estimated along vapour−liquid coexistence curve plotted as a function of temperature, T, for different system sizes, L. (a,b) Approach is demonstrated with n-butane confined in graphite and mica slit pore of 20 Å widths, respectively. The U_L is estimated at discrete temperatures in the range $340\,\text{K} \leq T \leq 360\,\text{K}$.

further indicates that the critical temperature estimated using simplified form of scaling law is statistically fairly close to the critical temperature estimated using more rigorous and computationally intensive technique of fourth-order Binder cumulant approach for the studied monoatomic model fluid.

Inspired with the fairly close estimates of critical temperature of confined monoatomic fluid, we studied the accuracy of critical temperature estimated for more complex confined fluids, such as n-alkanes, in the previous work [2] using simplified form of scaling law of density. Figure 2(a),(b) shows the critical temperature estimation of n-butane confined in graphite (G) and mica (M) slit pore, respectively, of width 20 Å using fourth-order cumulant approach. Critical temperatures estimated using cumulant approach, for n-butane confined in graphite and mica slit-pores, are 342.6 ± 1.6 and 341.4 ± 1.4 K, respectively, as also reported in Table 1.

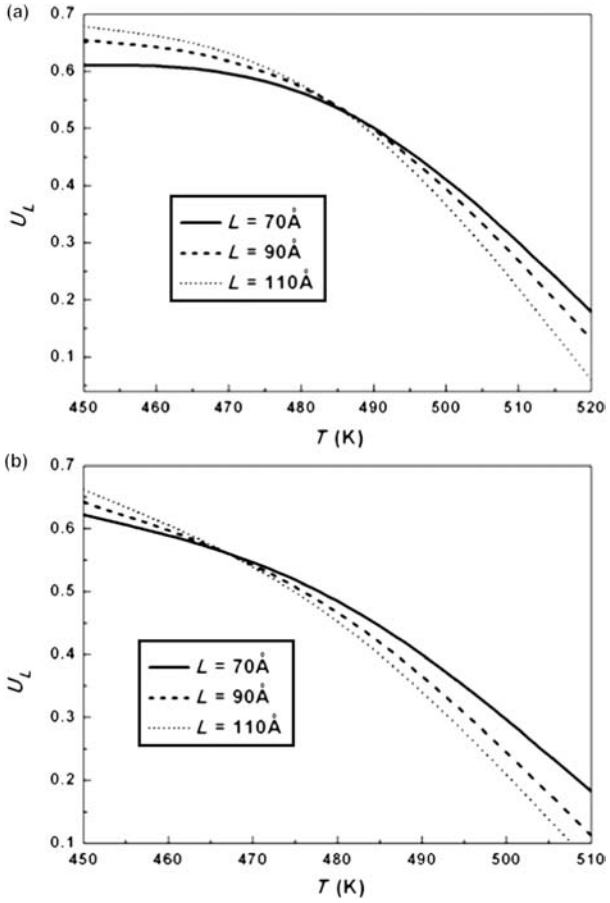

Figure 3. The fourth-order cumulants, U_L of order parameter, estimated along vapour–liquid coexistence curve plotted as a function of temperature, T, for different system sizes, L. (a,b) Approach is demonstrated with n-octane confined in graphite and mica slit pore of 30 Å widths, respectively. The U_L is estimated at discrete temperatures in the range $450\,\mathrm{K} \leq T \leq 520\,\mathrm{K}$ and $450\,\mathrm{K} \leq T \leq 510\,\mathrm{K}$ for the cases (a) and (b), respectively.

As can be seen from Table 1, the difference in the critical temperature estimation, using simplified form of scaling law [2] and the cumulant approach, for n-butane confined in graphite and mica slit pore is around 2.16% and 1.73%, respectively. Further, cumulant technique is employed to investigate and compare the critical temperature estimation of confined n-octane. Figure 3(a),(b) displays the critical temperature of n-octane confined in graphite (G) and mica (M) slit pore, respectively, of width 30 Å, using fourth-order cumulant approach. This investigation shows that the critical temperatures estimated for n-octane confined in graphite and mica slit pores are 486.2 ± 1.8 and 467.8 ± 2.1 K, respectively. As can be seen from Table 1, the difference in the critical temperature estimation of confined n-octane, using simplified form of scaling law reported in earlier work [2] and using cumulant approach, is only around 1.23% and 3.18%, respectively. Thus, these comparative investigations suggest that, even with chain molecules, such as n-alkane confined in slit pore geometry, the simplified form of scaling law gives fairly reasonable estimates of the critical temperature when compared with the more rigorous and computationally intensive approach of fourth-order Binder cumulant.

4. Conclusions

In summary, we have carried out extensive simulations using GC-TMMC technique and calculated fourth-order Binder cumulants along the vapour–liquid coexistence curve for simple spherical and chain-like molecules, confined in slit pore geometry of different attractive strengths. Undoubtedly, the critical temperature estimated using fourth-order cumulant approach provides more accurate estimates, because, in this approach, estimation of T_c is not biased by any assumptions about critical exponents. Moreover, as compared to the more rigorous cumulant approach, critical temperature estimated by simplified form of scaling law has shown overestimation of less than 3.2% for the studied systems in this work. This indicates that critical temperature estimation of studied bulk and confined system using GC-TMMC approach in conjunction with histogram reweighting technique and simplified form of scaling law provides fairly good estimate, provided the simulations performed with reasonable system sizes and in appropriate temperature ranges, depending on the pore width under investigation, as reported in the previous work [2,3].

Table 1. Critical temperature, T_c data for square-well fluid and n-alkanes estimated using two different techniques.

Square-well			n-Alkane			
System	T_c from simplified form of scaling law	T_c from fourth-order cumulant approach		System (Å)	T_c from simplified form of scaling law (K)	T_c from fourth-order cumulant approach (K)
Bulk	1.219 ± 0.001	1.217 ± 0.002	n-Butane	G/20	350.0 ± 1.0	342.6 ± 1.6
$H = 8$	1.091 ± 0.004	1.097 ± 0.006		M/20	347.3 ± 1.2	341.4 ± 1.4
$H = 2$	0.745 ± 0.002	0.734 ± 0.001	n-Octane	G/30	492.2 ± 1.6	486.2 ± 1.8
				M/30	482.7 ± 2.1	467.8 ± 1.9

Notes: Standard deviation with 67% confidence limit of the estimated T_c is reported on the basis of three different simulations run for each system. Here, G and M represent graphite and mica slit pores, respectively, for two different slit widths, H, 20 and 30 Å.

Acknowledgements

This work was supported by the Department of Science and Technology, Government of India (Grant no. SR/S3/CE/061/2009).

Notes

1. Current address: Department of Chemical Engineering, Thapar University, Patiala 147004, India.
2. Email: jayantks@iitk.ac.in

References

[1] K. Binder, *Computer simulations of critical phenomena and phase behaviour of fluids*, Mol. Phys. 108 (2010), pp. 1797–1815.
[2] S.K. Singh, A. Sinha, G. Deo, and J.K. Singh, *Vapor–liquid phase coexistence, critical properties, and surface tension of confined alkanes*, J. Phys. Chem. C 113 (2009), pp. 7170–7180.
[3] S.K. Singh, A.K. Saha, and J.K. Singh, *Molecular simulation study of vapor–liquid critical properties of a simple fluid in attractive slit pores: Crossover from 3D to 2D*, J. Phys. Chem. B 114 (2010), pp. 4283–4292.
[4] A.Z. Panagiotopoulos, *Direct determination of phase coexistence properties of fluids by Monte Carlo simulation in a new ensemble*, Mol. Phys. 61 (1987), pp. 813–826.
[5] N.B. Wilding, *Critical-point and coexistence-curve properties of the Lennard-Jones fluid: A finite-size scaling study*, Phys. Rev. E 52 (1995), pp. 602–611.
[6] N.B. Wilding and A.D. Bruce, *Density fluctuations and field mixing in the critical fluid*, J. Phys. Condens. Matter 4 (1992), pp. 3087–3108.
[7] J.E. Hunter and W.P. Reinhard, *Finite size scaling behavior of the free energy barrier between coexisting phases: Determination of the critical temperature and interfacial tension of the Lennard Jones fluid*, J. Chem. Phys. 103 (1995), pp. 8627–8637.
[8] J.M. Caillol, *Critical-point of the Lennard-Jones fluid: A finite-size scaling study*, J. Chem. Phys. 109 (1998), pp. 4885–4893.
[9] Y. Liu, A.Z. Panagiotopoulos, and P.G. Debenedetti, *Finite-size scaling study of the vapor–liquid critical properties of confined fluids: Crossover from three dimensions to two dimensions*, J. Chem. Phys. 132 (2010), pp. 144107–144116.
[10] J.K. Singh, J. Adhikari, and S.K. Kwak, *Vapor–liquid phase coexistence curves for Morse fluids*, Fluid Phase Equilb. 248 (2006), pp. 1–6.
[11] K. Binder, *Critical properties from Monte Carlo coarse graining and renormalization*, Phys. Rev. Lett. 47 (1981), pp. 693–696.
[12] W. Rżysko, A. Patrykiejew, S. Sokolowski, and O. Pizio, *Phase behavior of a two-dimensional and confined in slitlike pores square-shoulder, square-well fluid*, J. Chem. Phys. 132 (2010), pp. 164702–164712.
[13] W. Rzysko and M. Borowko, *A critical behavior of the Lennard-Jones dimeric fluid in two-dimensions: A Monte Carlo study*, Surf. Sci. 605 (2011), pp. 1219–1223.
[14] J. Pérez-Pellitero, P. Ungerer, and A.D. Mackie, *Effective critical point location: Application to thiophenes*, Mol. Simul. 33 (2007), pp. 777–785.
[15] A.S. Paluch, V.K. Shen, and J.R. Errington, *Comparing the use of Gibbs ensemble and grand-canonical transition-matrix Monte Carlo methods to determine phase equilibria*, Ind. Eng. Chem. Res. 47 (2008), pp. 4533–4541.
[16] J.K. Singh and S.K. Kwak, *Surface tension and vapor–liquid phase coexistence of confined square-well fluid*, J. Chem. Phys. 126 (2007), pp. 24702–24709.
[17] J.R. Errington, *Direct calculation of liquid-vapor phase equilibria from transition matrix Monte Carlo simulation*, J. Chem. Phys. 118 (2003), pp. 9915–9925.
[18] J.R. Errington and A.Z. Panagiotopoulos, *A new intermolecular potential model for the* n*-alkane homologous series*, J. Phys. Chem. B 103 (1999), pp. 6314–6322.
[19] W.A. Steele, *The physical interaction of gases with crystalline solids: I. Gas–solid energies and properties of isolated adsorbed atoms*, Surf. Sci. 36 (1973), pp. 317–352.
[20] J.P. Ryckaert and A. Bellemans, *Molecular dynamics of liquid* n*-butane near its boiling point*, Chem. Phys. Lett. 30 (1975), pp. 123–125.
[21] F. Wegner, *Corrections to scaling laws*, Phys. Rev. B 5 (1972), pp. 4529–4536.
[22] S.K. Singh and J.K. Singh, *Effect of pore morphology on vapor–liquid phase transition and crossover behavior of critical properties from 3D to 2D*, Fluid Phase Equilib. 300 (2011), pp. 182–187.
[23] W. Rżysko, O. Pizio, A. Patrykiejew, and S. Sokolowski, *Phase diagram of a square-shoulder, square-well fluid revisited*, J. Chem. Phys. 129 (2008), pp. 124502–124504.